Sulfur doping of diamond films: Spectroscopic, electronic, and gas-phase studies

James R. Petherbridge, Paul W. May,[a] Gareth M. Fuge, Giles F. Robertson, Keith N. Rosser, and Michael N. R. Ashfold
School of Chemistry, University of Bristol, Bristol BS8 1TS, United Kingdom

(Received 2 July 2001; accepted for publication 12 December 2001)

Chemical vapor deposition (CVD) has been used to grow sulfur doped diamond films on undoped Si and single crystal HPHT diamond as substrates, using a 1% CH_4/H_2 gas mixture with various levels of H_2S addition (100–5000 ppm), using both microwave (MW) plasma enhanced CVD and hot filament (HF) CVD. The two deposition techniques yield very different results. HFCVD produces diamond films containing only trace amounts of S (as analyzed by x-ray photoelectron spectroscopy), the film crystallinity is virtually unaffected by gas phase H_2S concentration, and the films remain highly resistive. In contrast, MWCVD produces diamond films with S incorporated at levels of up to 0.2%, and the amount of S incorporation is directly proportional to the H_2S concentration in the gas phase. Secondary electron microscopy observations show that the crystal quality of these films reduces with increasing S incorporation. Four point probe measurements gave the room temperature resistivities of these S-doped and MW grown films as $\sim 200\ \Omega$ cm, which makes them ~ 3 times more conductive than undoped diamond grown under similar conditions. Molecular beam mass spectrometry has been used to measure simultaneously the concentrations of the dominant gas phase species present during growth, for H_2S doping levels (1000–10 000 ppm in the gas phase) in 1% CH_4/H_2 mixtures, and for 1% CS_2/H_2 gas mixtures, for both MW and HF activation. CS_2 and CS have both been detected in significant concentrations in all of the MW plasmas that yield S-doped diamond films, whereas CS was not detected in the gas phase during HF growth. This suggests that CS may be an important intermediary facilitating S incorporation into diamond. Furthermore, deposition of yellow S was observed on the cold chamber walls when using H_2S concentrations >5000 ppm in the MW system, but very little S deposition was observed for the HF system under similar conditions. All of these results are rationalized by a model of the important gas phase chemical reactions, which recognizes the very different gas temperature profiles within the two different types of deposition reactor.
[DOI: 10.1063/1.1448679]

I. INTRODUCTION

The many extreme physical and mechanical properties[1,2] of thin film diamond grown by chemical vapor deposition (CVD) have led to interest in such films for use in electronic devices. Such devices would be mechanically durable and also present less of a heat management problem than silicon based examples because of the high thermal conductivity of diamond. Boron doped CVD diamond films with *p*-type semiconductor properties are grown routinely by the addition of B-containing gases such as diborane to the standard CVD gas mixture (1% CH_4/H_2).[3] Such films find use in UV detectors[4] and as electrodes for harsh electrochemical applications (e.g., highly acidic solutions).[5] However, obtaining *n*-type semiconducting diamond films by CVD has proved more challenging, mainly due to the fact that suitable donor atoms (e.g., P, O, and As) are larger than carbon, making incorporation into the diamond lattice unfavorable. Nitrogen readily incorporates into CVD diamond films during growth, but the resulting donor levels are too deep (1.7 eV) for many electronic applications.[6] Phosphorus doped diamond films exhibiting *n*-type semiconductor properties have been grown,[7] but again, these exhibit poor conductivity and crystal quality making them unsuitable for some device applications.[8]

The technique of ion implantation using donor elements such as Li, Na, and P has been utilized in unsuccessful attempts[9,10] to obtain diamond films with *n*-type semiconducting properties. However, Hasegawa *et al.*[11] report that sulfur ion implantation in CVD homoepitaxial diamond (100) films leads to *n*-type conductivity, as demonstrated by Hall effect measurements. This group also fabricated a *p*-*n* junction by combining *p*-type (B doped by CVD) and *n*-type (sulfur doped by ion implantation) homoepitaxial diamond and confirmed its characteristics by $I-V$ and $C-V$ measurements.

Barber and Yarbrough[12] have shown that diamond growth is possible using mixtures of a few percent CS_2 diluted in hydrogen, within a hot filament CVD (HFCVD) reactor. Although no electronic measurements were conducted, their work has encouraged several subsequent investigations of H_2S as another possible source of sulfur for *in situ* doping of CVD diamond films.

[a]Author to whom correspondence should be addressed; electronic mail: paul.may@bris.ac.uk

Microwave plasma enhanced CVD (MPCVD) has been reported by Sakaguchi *et al.*[13–15] to yield semiconducting, homoepitaxial diamond films exhibiting *n*-type behavior by H_2S addition to the 1% CH_4/H_2 gas mixture. They found that small H_2S additions ($\sim$100 ppm) improved crystallinity, but further increases in H_2S concentrations led to a decrease in crystallinity. Film growth rate was also seen to decrease with increased H_2S addition, however, the quality of the films (as measured by Raman spectroscopy) was found to be relatively insensitive to changes in H_2S addition. Hall mobilities for films produced using H_2S doping levels of 50–100 ppm were found to be relatively high ($597\ cm^2\ V^{-1}\ S^{-1}$), suggesting that doping with S by this method might finally prove to be the route to *n*-type CVD diamond with useful electronic properties.

More recently, however, another group[16] repeated measurements on these samples and attributed this mobility to the presence of boron impurities within the film. They also found that the sign of the charge carriers was positive (i.e., the films exhibited *p*-type, not *n*-type semiconducting properties). However, the NIRIM group still maintain that their samples are truly *n* type, and have backed up this claim with further samples (which do not contain B) and Hall measurements made in independent laboratories which give the required negative coefficient.[17] Nevertheless, it is fair to say that there is still some controversy surrounding the ability of H_2S doping to produce *n*-type conducting CVD diamond.

Most of the work involving *n*-type doping of CVD diamond has focused on the electronic properties of the resultant films, rather than the gas phase chemistry leading to deposition. Dandy[18] presented simple thermodynamic equilibrium calculations for $H_2S/CH_4/H_2$ gas mixtures, and concluded that the probable sulfur precursor dopant species was the SH radical, rather than the more stable species CS. To date, however, no experimental measurements of gas phase species concentrations present during the growth of sulfur doped CVD diamond films from H_2S have yet been reported.

Molecular beam mass spectroscopy (MBMS) is a powerful technique for carrying out such measurements. Hsu[19] pioneered the use of MBMS to investigate diamond MWCVD using CH_4/H_2 gas mixtures. In his experiment, the gas was sampled via an orifice in the substrate, allowing analysis of the composition of the flux incident to the diamond growing surface. Later work in our group used MBMS to sample gas directly from the plasma, thus probing the gas phase chemistry in isolation, with minimum perturbation from gas–surface reactions. We have used this powerful technique to obtain absolute mole fractions of the gas phase species present in both hot filament[20–23] and microwave systems[24–26] for a variety of gas mixtures and dopant gas additions. We now report the results of using MBMS to make *in situ* measurements of species mole fractions, as a function of both input gas composition and temperature, for both microwave (MW) and hot filament (HF) activation of the gas phase chemistry, using gas mixtures suitable for producing S-doped diamond.

II. EXPERIMENT

A. Growth experiments: Hot filament CVD

The deposition chamber was a standard hot filament CVD reactor employing a coiled 0.25-mm-thick Ta filament (maintained at $\sim$2200 °C) to activate the gas mixture. The substrate was placed 5 mm below the filament on a heated substrate holder (900 °C). The chamber pressure was 20 Torr and duration of growth was 8 h. The feedstock gases used were H_2 (99.999% purity), CH_4 (99.999% purity), and H_2S (99.5% purity). To obtain gas phase H_2S levels below 1000 ppm, a cylinder of 1% H_2S in H_2 was employed and further diluted by use of appropriate flow rate ratios regulated by mass flow controllers. Total gas flow was maintained at 200 sccm.

Films were deposited on both *p*-doped (resistivity $\sim 1-10\ \Omega$ cm) and undoped single crystal (100) silicon wafers (resistivity $\sim 2.3\times 10^5\ \Omega$ cm), manually preabraded with 1–3 μm diamond grit. All deposition runs reported here used a 1% CH_4/H_2 gas mixture with H_2S additions over the range 0–5000 ppm.

B. Growth experiments: Microwave plasma CVD

Diamond deposition was performed using a 1.5 kW ASTeX-style 2.45 GHz microwave plasma CVD reactor. The double-walled chamber was water-cooled and contained a Mo substrate holder. For experiments using H_2S or CS_2 additions, this Mo substrate holder was covered using a blank Si wafer, since it has been reported that hot Mo possibly acts as a sink for gas phase S species, scavenging them and reacting to form solid MoS_2.[17] Substrates (as outlined above) were placed on an alumina plate on top of this Si cover wafer and were thus elevated about 1 mm into the plasma, enabling automatic heating of the substrate to $\sim$900 °C (as measured by a two color optical pyrometer). The chamber pressure was 40 Torr with an applied microwave power of 1 kW, with deposition lasting 8 h. In addition to the H_2S/1% CH_4/H_2 mixtures outlined above, experiments were performed using a 0.5% CS_2/H_2 gas mixture (using the vapor pressure above a liquid sample of CS_2). All the films were exposed to a 10 min hydrogen plasma after growth to ensure a consistent H-terminated surface suitable for reproducible electrical measurements.

It is important to mention that neither the HF reactor mentioned earlier, nor the MW chamber had ever been used for processing boron-containing samples, nor had any B-containing gases ever been introduced into them. Thus they were completely B-free, so removing the chance of accidental contamination of the samples with B.

C. Film analysis

Films were examined using scanning electron microscopy (SEM) to determine crystal morphology and thickness and by 514.5 nm (Ar^+) laser Raman spectroscopy (LRS) to assess film quality. The HF-grown films were analyzed by x-ray photoelectron spectroscopy (XPS) at NIRIM using Al $K\alpha$ excitation, whereas the MW-grown films were analyzed in Bristol using Mg $K\alpha$ excitation. Charging of insu-

lating films was minimized by use of an electron flood gun, and any remaining charging effects were counteracted by offsetting the energy scale with respect to the known values for carbon peaks. The absolute values for the sulfur content (i.e., S:C ratio) of the films was calculated by comparison of the areas of selected S peak(s) and C peak(s), following calibration using the sensitivity factors[27] appropriate for each element. Films were also analyzed by secondary ion mass spectrometry (SIMS)[28] to check for impurities such as B which might affect the electrical properties of the film.

The resistivity of the films was determined by four point probe[29] measurements. Being a technique which relies upon surface contacts, this will measure the surface conductivity of diamond, rather than the conductivity through the bulk. Care was therefore taken to ensure that the surface properties of each of the diamond samples was treated identically during deposition, so that any changes in surface conductivity would be due to the presence of S within the film and not processing variations. The values of sheet resistance obtained by this method (following the procedure outlined in Ref. 29), were typically in the range 10^5-10^6 Ω square^{-1}, and were then converted to film resistivity by multiplying by the film thickness as measured by cross-sectional SEM.

Hall effect measurements (at Bath University, Cambridge University, and University College London) were also attempted in order to determine the semiconducting properties of the films. Previous experience with Hall measurements showed that S-doped films grown epitaxially on single crystal (HPHT) diamond substrates were dominated by the conductivity of the substrate, which was slightly semiconducting due to B or N impurities. Therefore all Hall measurements were made using films grown on high resistivity undoped Si in order to prevent the substrate from influencing the results. This does mean, though, that care should be taken when comparing the electrical results of our polycrystalline heteroepitaxially grown diamond films with those from single-crystal epitaxially grown films reported elsewhere.[13–15]

D. MBMS

A full description of the MBMS system and gas sampling technique has been published previously,[24] but a brief outline will be given here. A two stage differential pumping system was used to sample gas (at 20 Torr) from the side of the microwave plasma ball (or at a distance of 5 mm from the hot filament) via an orifice (~ 100 μm diameter) in a sampling cone. Although such an intrusive method is bound to perturb the plasma, the fact that the position of the plasma ball and the reflected microwave power level are insensitive to the presence of the probe suggest that this perturbation is minimal. Gas passing through this orifice experienced a pressure differential ($20 \rightarrow 10^{-3}$ Torr) and underwent adiabatic expansion, forming a molecular beam in which chemical reactions were effectively frozen out. The molecular beam then passed through a collimating skimmer into a quadrupole mass spectrometer (Hiden Analytical) maintained at $\sim 10^{-6}$ Torr, whereupon gas phase species were ionized by electron impact. The electron ionization energy is user-selectable in the range 4–70 eV. The electron ionizer energies used to detect each species were H_2, CH_4 and CS_2 16.0 eV, C_2H_2 13.2 eV (to minimize contributions to the $m/e = 26$ signal due to the cracking of C_2H_4 occurring above 13.5 eV), H_2S 13.2 eV, CS 13.6 eV (to minimize signal from CO_2 occurring above 13.8 eV), and CH_3 13.6 eV (to reduce signal from cracking of CH_4 above 14.3 eV).

All MBMS experiments were performed in the microwave chamber, first with gas being sampled from the microwave plasma ball, and then, after modifications to the apparatus, from the area surrounding a filament analogous to that used in the HF growth experiments, outlined above. During the latter studies, the filament temperature was monitored via a two color optical pyrometer. Two sets of experiments were performed in which measurements of species mole fractions were made in both the MW and HF activation environments. First, H_2S (0–10 000 ppm) was added to a 1% CH_4/H_2 gas mixture keeping the filament temperature, T_{fil}, and MW power constant at 2200 °C and 1 kW, respectively. Second, a 1% CS_2/H_2 mixture was introduced into the chamber, and either the temperature of the HF or the applied MW power was varied. The effect of varying T_{fil} on species mole fractions was also investigated for a 0.5% H_2S/1% CH_4/H_2 gas mixture. The chamber pressure for all MBMS experiments was 20 Torr and in all cases (MW or HF) the probe was positioned at the same radial distance (from either the center of the MW plasma or the HF) as the substrate during deposition.

Data collected from the mass spectrometer were converted into mole fraction values, the correction and calibration procedures being identical to those used in previous MBMS studies.[20–25]

III. RESULTS

A. Hot filament deposition results

Figures 1(a)–1(c) show that there is little change in film morphology between samples deposited with 100, 6000, and 10 000 ppm H_2S addition to a HF activated 1% CH_4/H_2 gas mixture. All films exhibit well-defined microcrystalline facets. There was also no significant change in film growth rate with increased input H_2S, as illustrated by Fig. 2. No evidence for S incorporation was found for any of the films when examined by SIMS. However, for films grown using a gas phase H_2S concentration of >6000 ppm, XPS analysis revealed trace amounts of S present, but the size of the signal associated with the sulfur $2p$ peaks at 162 and 163 eV was too small to allow the S content to be quantified accurately. These peaks were found to be shifted by 6 eV (from the average literature value for S-containing molecules of 162 eV) to 169 eV. This is a much larger shift than has been previously reported, which are normally between 1 and 2 eV from the average value depending upon the exact environment of the S within the molecule. We note that XPS averages the signal over the whole area of the substrate (1 cm^2), and so the position of the S within the film cannot be determined. Depth profiling, however, shows that the S is uniformly distributed throughout the film thickness, and is not just present at the surface, but the spatial resolution of the

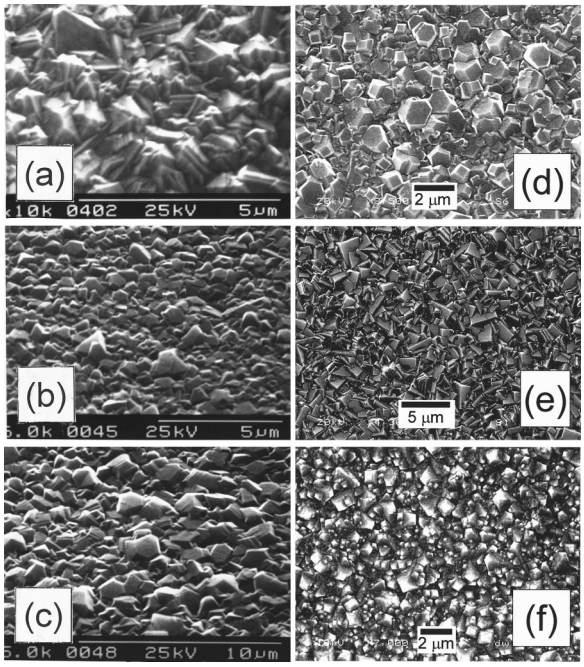

FIG. 1. SEM micrographs for films grown using 1% CH_4/H_2 gas mixtures with H_2S additions of (a) 100, (b) 6000, and (c) 10 000 ppm in a HF reactor, and (d) 100, (e) 1000, and (f) 5000 ppm additions in a MW plasma reactor. Conditions: total gas flow 200 sccm, growth time 8 h, substrate temperature 900 °C, pressure 20 Torr (HF) and 40 Torr (MW), and 1 kW applied microwave power or filament temperature of 2200 °C.

technique is insufficient to determine if the S is concentrated in say, grain boundaries. As expected, neither XPS nor SIMS showed any evidence of B contamination. Hall effect measurements proved unsuccessful due to the high room temperature resistivity of these films ($\sim 300\ \Omega$ cm) so it is therefore still unclear what the semiconducting properties (if any) of these samples are. The main conclusions seem to be that these levels of HF activation do not provide a route to making S-doped diamond films.

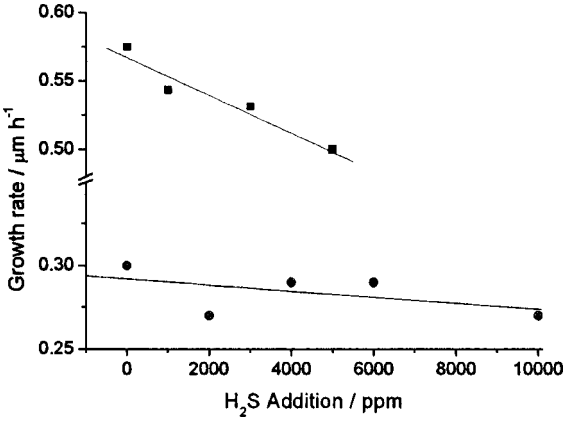

FIG. 2. Film growth rate (measured by cross-sectional SEM) vs H_2S addition for films grown in H_2S/1% CH_4/H_2 gas mixtures. (●) HF and (■) MW deposited films, with other process conditions as for Fig. 1. The lines are least-square fits to linear functions.

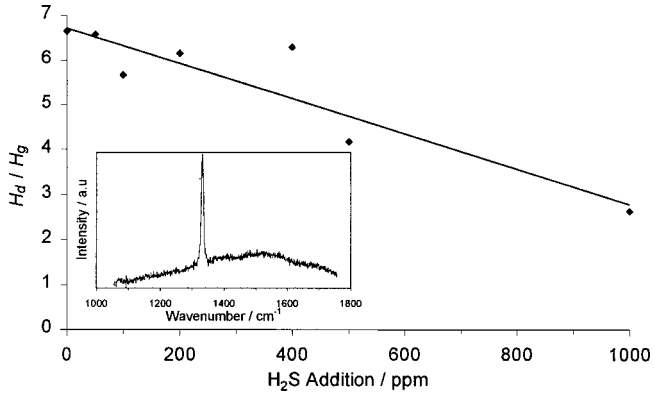

FIG. 3. Plot of film quality vs H_2S addition for films deposited from a 1% CH_4/H_2 MW plasma. The insert shows the laser Raman spectrum (514.5 nm excitation) for a sample grown using 5000 ppm input H_2S. Film quality (i.e., the ratio of sp^3:sp^2 carbon bonding) is defined as the ratio of the height of the diamond peak at 1332 cm^{-1}, H_d, to the height of the graphite band at 1550 cm^{-1}, H_g. Both heights are measured relative to an (estimated) underlying spectral background attributed to photoluminescence. Other conditions as given in Fig. 1.

B. Microwave plasma deposition results

In contrast with the films grown by HF deposition, Figs. 1(d)–1(f) show that for MW deposited samples there is a pronounced variation in film morphology with increased H_2S input level. Increasing the H_2S input levels from 100 to 1000 ppm [Figs. 1(d) and 1(e)] significantly increases the proportion of (100) oriented facets, whereas further increasing H_2S levels to 5000 ppm [Fig. 1(f)] results in the crystal facets taking on a rounded appearance. It was also observed that additions of over 1000 ppm H_2S to the plasma caused the deposition of a layer ($\sim$0.5-mm-thick after a few hours) of yellow powdery sulfur on the colder parts of the chamber, such as the walls and windows. Although S deposition was also encountered during the HF growth experiments, it only occurred with the highest H_2S concentrations (above 5000 ppm), and the rate of deposition was estimated to be about ten times smaller than that seen in the MW system. Some of this difference in behavior may be attributable to the lower total power levels in the HF system (300 W) compared to the MW system (1 kW) but it also hints at significant differences in the gas phase chemistry between the two systems.

Figure 2 illustrates the fall in film growth rates with increased H_2S levels. This observation has been made by others[15] but over a smaller range of H_2S concentrations, although the reported effect was more pronounced. The quality of the diamond films was measured by LRS, as presented in Fig. 3. Here the quality of the films (i.e., the ratio of sp^3:sp^2 carbon bonding) is taken to be the ratio of the height of the diamond peak at 1332 cm^{-1}, H_d, to the height of the graphite band at 1550 cm^{-1}, H_g. Both heights are measured relative to an (estimated) underlying spectral background attributed to photoluminescence.[30] The photoluminescence background did not show any evidence for N–V centers at 575 or 637 nm, indicating no inadvertent contamination of the films by nitrogen. Figure 3 shows a decline in film quality with increased H_2S addition, although it should be noted that even the most highly doped sample (5000 ppm H_2S

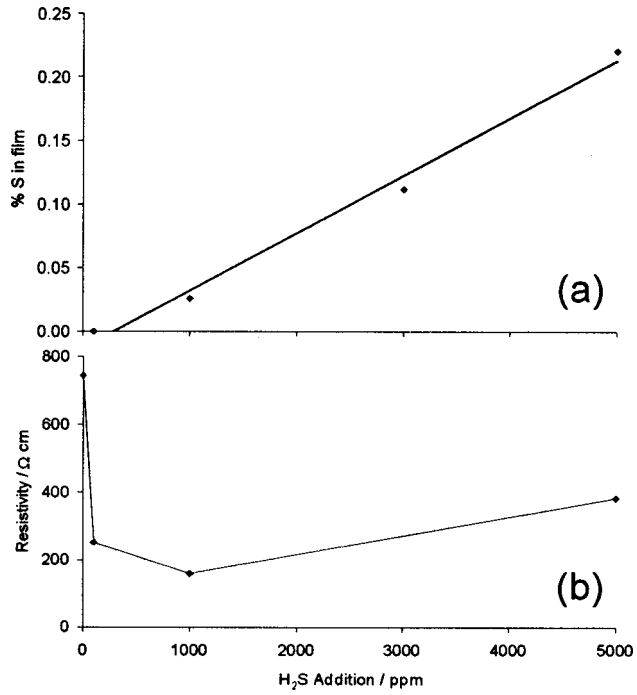

FIG. 4. Plots of (a) %S content (as measured by XPS) and (b) resistivity (as measured by four point probe) of films vs H_2S addition to a 1% CH_4/H_2 MW plasma.

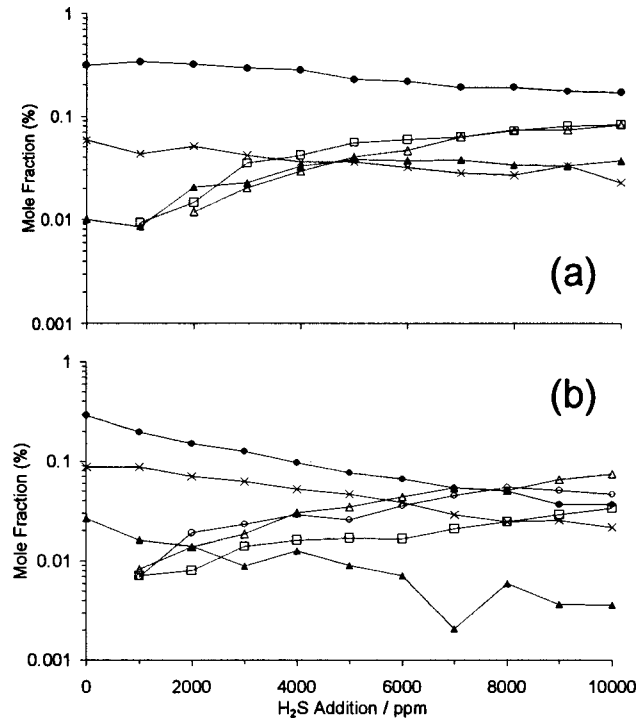

FIG. 5. MBMS results of species mole fraction vs H_2S addition to a 1% CH_4/H_2 gas mixture for gas sampled from (a) a distance of 5 mm from a hot filament and (b) the edge of a MW plasma ~23 mm from the plasma center. Conditions: 20 Torr, 1 kW applied microwave power and filament temperature of 2200 °C. (●) CH_4, (×) C_2H_2, (▲) CH_3, (□) H_2S, (△) CS_2, and (○) CS.

addition) is still found to be of high quality, as indicated by the presence of a pronounced diamond peak in its Raman spectrum shown in the inset.

Figure 4(a) shows XPS results for MW grown films. A linear increase in the %S detected in the films with increased H_2S concentrations is seen, although only for dopant levels over 100 ppm (since below this value the S in the films was below the XPS detection limit). The sulfur $2p$ peak (compared to the literature value) for all films was observed to be shifted by ~1 eV to higher energy. This is a much smaller shift than was seen for the HF deposited film (with 6000 ppm H_2S in the gas phase), suggesting that S may be present in different bonding forms in the two types of sample. Sulfur is present in much higher levels in the films grown using MW activation compared to those grown using HF activation, with values up to 0.2% being obtained. However, Fig. 4(a) also shows that even at this level the S/C ratio in the deposited films is only ~1/200 that in the input gas mixture; the remainder is presumably pumped away or depositing as solid S on the walls of the reactor. Again, neither XPS nor SIMS showed any evidence of contamination by B or other unexpected n- or p-dopant atoms.

Four point probe measurements of film resistivity at room temperature are presented in Fig. 4(b) and show the films to have significant resistance with values which are in the range usually observed for as-deposited or H-terminated CVD diamond films.[31] This may reflect the defective, polycrystalline nature of these heteroepitaxially grown films. A clear drop in resistivity is observed between undoped (744 Ω cm) and doped samples (100 and 1000 ppm H_2S, ~200 Ω cm). The small rise in resistivity between the 1000 and 5000 ppm H_2S samples is probably due to the presence of additional grain boundaries containing impurities in the more highly doped films. Unfortunately, Hall effect measurements proved unsuccessful due to the high resistivity of these films, so the semiconducting properties of these samples remain unclear.

A film was also grown on Si using a 0.5% CS_2/H_2 gas mixture. The film was found to give a clear diamond Raman peak at 1332 cm^{-1} and exhibited good crystallinity [identical in appearance to that shown in Fig. 1(e)]. Although sulfur was detected in the film (at an S/C ratio of ~0.16% as measured by XPS, i.e., an S/C ratio only ~1/1000 that in the input gas mixture), four point probe measurements showed the sample to be significantly more resistive than the S-doped examples from H_2S/1% CH_4/H_2 gas mixtures, suggesting that a little S incorporation into the lattice had occurred. As for H_2S additions, a layer of S was deposited on the cool chamber walls.

C. MBMS

Figure 5 shows how the mole fractions of the species: CH_4, CH_3, C_2H_2, H_2S, CS_2, and CS vary with increased H_2S addition (0–10 000 ppm) for both (a) HF and (b) MW activation. In the HF experiment (sampling gas 5 mm from the filament maintained at 2200 °C), the CH_4 and C_2H_2 mole fractions both reduce slightly with increased H_2S addition [as shown in Fig. 5(a)], whereas the mole fractions of H_2S and CH_3 rise. Unsurprisingly, the mole fraction of H_2S measured in the gas phase is found to be proportional to the input concentration of H_2S in the feedstock gas mixture. At higher

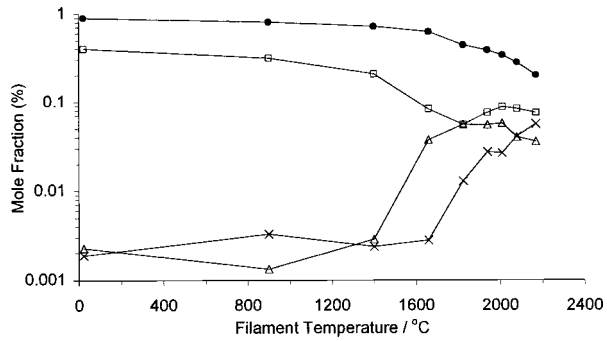

FIG. 6. MBMS plots of species mole fraction vs filament temperature for a 0.5% H_2S/1% CH_4/H_2 gas mixture. The gas was sampled at a distance of 5 mm from the filament and the pressure was maintained at 20 Torr. (●) CH_4, (×) C_2H_2, (□) H_2S, and (△) CS_2.

H_2S input fractions, CS_2 is also present as a result of gas phase reactions, but the CS radical is not detected. In contrast, the addition of H_2S into a 1% CH_4/H_2 MW plasma [Fig. 5(b)] causes a significant reduction in CH_4, C_2H_2, and CH_3 mole fractions. H_2S and CS_2 are seen to rise with increased H_2S addition with a measured CS_2/H_2S ratio of ~ 2, and significant amounts of CS are now measured, in quantities comparable to those from CS_2.

Returning to HF activation, the dependence of species mole fraction on T_{fil} is illustrated by Fig. 6. Mole fractions of both CH_4 and H_2S are seen to decrease for $T_{fil} > 1400\,°C$ whereas C_2H_2 and CS_2 concentrations rise in this temperature region.

Presented in Fig. 7 is the dependence of species mole fraction on (a) filament temperature and (b) applied microwave power, for a 1% CS_2/H_2 gas mixture. In the HF experiment a clear decrease in CS_2 concentrations is observed, along with a rise in H_2S, CH_4, and CH_3 mole fractions for $T_{fil} > 800\,°C$. Increasing applied microwave power, over the range illustrated by Fig. 7(b), has little effect on the relative concentrations of all species. Again CS_2 and H_2 react together to form H_2S, CH_4, C_2H_2, and CH_3. No measurable amounts of CS were detected in either of the CS_2/H_2 experiments. One interesting observation was that the CS_2/H_2 plasma was larger in size than a H_2S/1% CH_4/H_2 plasma (for the same applied microwave power). In all five MBMS experiments no detectable levels of SH, S, or S_2 were observed.

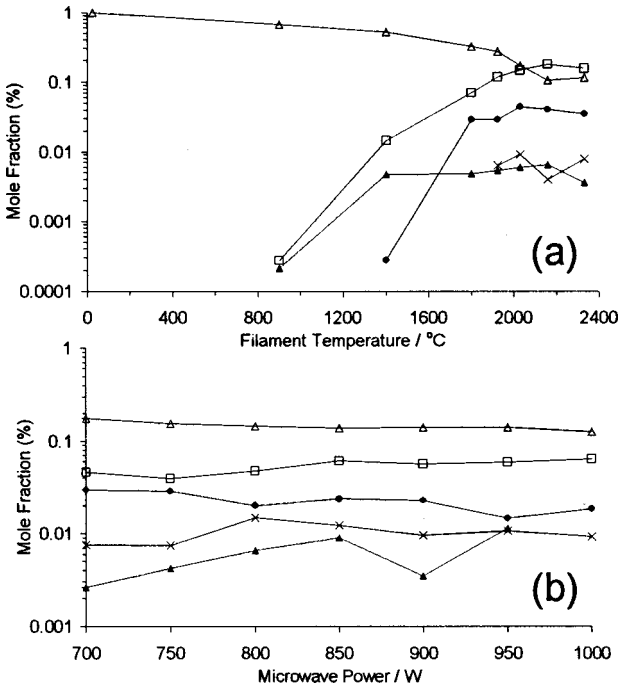

FIG. 7. MBMS plots of species mole fraction for a 1% CS_2/H_2 gas mixture measured for various (a) filament temperatures and (b) applied microwave powers. Other conditions and gas sampling details are as given in Fig. 5. (●) CH_4, (×) C_2H_2, (▲) CH_3, (□) H_2S, and (△) CS_2.

IV. DISCUSSION

H_2S addition to a 1% CH_4/H_2 mixture in these experiments is seen to have very different effects depending upon whether the mixture is HF or MW activated. For diamond grown in a HF reactor, the addition of trace amounts of H_2S has little effect on the crystallinity, growth rate, and quality of the films. Relatively high input levels (>5000 ppm H_2S) are required in order to obtain even trace amounts of S within the films, and the films remain highly electrically resistive. In contrast, MW plasma CVD allows the incorporation of larger amounts of S (as indicated by XPS) at low H_2S concentrations, although the incorporation efficiency is still low (i.e., the S/C ratio in the deposited films is only $\sim 1/200$ of that in the input gas mixture). The large XPS peak shift (6 eV) seen for the S-doped HF-deposited diamond film suggests that the trace amount of S present exists in an unusual bonding form that has not been seen in the XPS literature before. In contrast, the samples grown by MW deposition gave much smaller peak shifts (~ 1 eV), suggesting that the S environment is similar to that seen in other C–S bonded systems, such as polyethylene sulfide $(CH_2-S-CH_2)_n$. The fact that the HF and MW grown films were analyzed using Al ($K\alpha$) and Mg ($K\alpha$) excitation, respectively, might account for the difference in peak shifts observed (although this seems unlikely). It therefore seems that there is some significant difference between these two deposition methods as implemented here, which affects both the likelihood and nature of S inclusion into the diamond lattice.

Figure 5 shows a clear contrast in the gas phase chemistry between MW and HF activated CVD. In the HF system, upon addition of H_2S to the 1% CH_4/H_2 mixture, CS_2 is formed leading to a slight reduction in CH_4 (and therefore CH_3) concentrations. Importantly, the CS_2/H_2S ratio never exceeds unity and no CS is observed. In contrast, for MW plasmas the detected mole fraction of CS_2 is ~ 4 times that of H_2S at all H_2S additions. CS_2 and CS are detected in roughly equal amounts, and a much more significant reduction in CH_4, C_2H_2, and also CH_3 is observed, presumably because the "missing" carbon is locked up in this CS/CS_2 reservoir. As significant concentrations of CS are detected in the MW plasma (which facilitates S incorporation) but not in the region around the HF (which gives little S incorporation), we speculate that CS is the species responsible for the inclusion of S into the diamond films. The observed drop in CH_3

TABLE I. Selected reactions proposed for C/H/S gas mixtures within HF and MW diamond CVD reactors operating at ~20 Torr. Gibbs free energies of reaction, ΔG_{reac}, presented for 1100 and 1600 K are calculated using free energies of formation taken from Ref. 39. The data for reactions 7–10 were computed from CCSD(T)/cc-pVTZ//MP2/6-311G** electronic structure calculations, with free energy corrections derived from the standard methods of statistical mechanics, together with MP2/6-311G** rotational constants and vibrational frequencies (see Ref. 40). A conservative error estimate for this procedure is 40 kJ mol^{-1}

	Reaction	ΔG_{reac}/(kJ mol^{-1}) 1100 K	1600 K
1	$CH_4+2H_2S \leftrightharpoons CS_2+4H_2$	23.6	−85.0
2	$CS_2+H \leftrightharpoons CS+HS$	−4.6	−59.2
3	$HS+H \leftrightharpoons S+H_2$	−31.0	10.9
4	$2HS \leftrightharpoons S_2+H_2$	−42.6	43.2
5	$H_2S+H \leftrightharpoons HS+H_2$	−102.4	−140.9
6	$CH_4+H \leftrightharpoons CH_3+H_2$	−28.2	−42.6
7	$CH_3+HS \leftrightharpoons CH_3SH$	−125.0	−55.6
8	$CH_3SH \leftrightharpoons CS+2H_2$	21.0	−99.1
9	$CH_3SH+H \leftrightharpoons CH_4+SH$	−142.9	−138.4
10	$CH_3SH+H \leftrightharpoons CH_3S+H_2$	−83.3	−84.1
11	$CS+H_2S \leftrightharpoons CS_2+H_2$	−97.8	−81.8

mole fraction with increased H_2S addition, the fall in MW deposited film growth rates, and the lack of such observations for the HF system are all to be expected given that CH_3 is believed to be the major diamond growth precursor in low pressure CVD reactors.[26,32,33]

The reaction of H_2S and CH_4 to form CS_2 is illustrated in Fig. 6 where, for an input gas mixture of 0.5% H_2S/1% CH_4/H_2, the reduction in CH_4 and H_2S concentrations and the increase in CS_2, C_2H_2, and CH_3 mole fractions with filament temperature are observed at $T_{fil}>1400\,°C$. The chemistry of these $H_2S/CH_4/H_2$ mixtures is summarized in Table I, where the major overall processes and individual step reactions are listed, along with their Gibbs free energies (ΔG_{reac}) at 1100 and 1600 K.

The dominant overall chemical process for these systems is reaction 1, in which CH_4 and H_2S are in equilibrium with CS_2 and H_2 (with ΔG_{reac} of 23.6 and -85.0 kJ mol^{-1} at 1100 and 1600 K, respectively). The equilibrium constant (the ratio of product/reactant concentrations) for reaction 1 is $K=0.076$ at a temperature of 1100 K and $K=595$ at 1600 K (given that $\Delta G_{reac}=-RT\ln K$).

$$CH_4+2H_2S \leftrightharpoons CS_2+H_2. \qquad \text{(reaction 1)}.$$

At the higher temperatures, CS_2 then reacts with atomic H producing CS and SH (reaction 2) leading to a buildup of CS, as seen for the MW system. Table I shows that reaction 1 (formation of CS_2 from H_2S and CH_4) is unfavorable (i.e., $\Delta G_{reac}>0$) at lower gas temperatures (T_{gas}). T_{gas} is known[34] to fall from ~2400 K at the HF to ~1800 K within a few μm, and to ~1100 K at a distance of 5 mm from the HF (from where the gas is probed by MBMS and where the substrate is located for diamond growth). In contrast, within a representative 1% CH_4/H_2 MW plasma the temperature does not vary considerably from the plasma center (T_{gas} ~2200 K)[35] outwards to the plasma edge (T_{gas}~1600 K for a radial distance of ~23 mm),[24] where gas is sampled in the MBMS experiments (and where the substrate is positioned for growth). The temperature gradient within a MW reactor is therefore much shallower compared to that around a HF reactor, and the volume of gas with a temperature sufficiently high to favor formation of CS_2 (through reaction 1) is substantially larger within the MW plasma. Reactions 1 and 2 can therefore create CS_2 and CS, respectively, throughout the entire plasma region, and both these species will be present in significant concentrations at the growing diamond surface. However, in the HF system, the temperature drop away from the filament is so severe that except for very close to the filament the equilibrium (1) lies towards the left-hand side, CS_2 production is inefficient and so, as a result, is CS production (reaction 2). Thus the growing diamond surface in a HF system will see only those species responsible for normal CVD diamond growth (CH_4, CH_3, H atoms, etc.), as well as some H_2S and CS_2, but little or no CS. This results in diamond growth in HF systems being relatively unaffected by H_2S addition and no S incorporation.

Another contrast between MW and HF deposition is the observation that for H_2S concentrations over 1000 ppm the former results in the deposition of a layer of sulfur powder on the cool chamber walls, whereas no such problem is encountered in the HF system. One possible explanation for this is that, in the MW plasma, the SH radicals which are formed in the plasma via reaction 2 then diffuse out to the cooler regions of the reactor and there react with H to form S and H_2 (as in reaction 3). Reaction 4 shows an alternative route to sulfur deposition in which SH radicals recombine to form S_2. In either case, the resulting (S or S_2) species may diffuse to, and deposit on, the chamber wall, or aggregate in the gas phase (catalyzed by the presence of a third body) to make larger S-containing clusters, prior to depositing onto the chamber walls. Evidence for this comes from the recent detection of excited S_2 radicals from H_2S and CS_2-containing MW plasmas using optical emission spectroscopy.[36] As discussed above, the production of CS (via reaction 2) and, with it, HS, is significantly larger within the MW plasma compared to the HF environment. The extra HS in the MW plasma relative to the HF environment leads to increased S and S_2 formation (via reactions 3 and 4) and consequently, increased deposition of sulfur.

Reaction 1 is an overall equilibrium consisting of many intermediate step reactions, in which the chemistry is initiated by H-abstraction from CH_4 and H_2S to form CH_3, SH, and H_2 (reactions 5 and 6). Both of these reactions are thermodynamically favored ($\Delta G_{reac}<0$) over the temperature range presented in Table I, although more so for H_2S due to the lower bond dissociation energy for the H–S bond (399 kJ mol^{-1}) compared with the C–H bond (435 kJ mol^{-1}).[37] The CH_3 and SH radicals may then couple to form the predicted species CH_3SH (reaction 7, $\Delta G_{reac}<0$ for $T_{gas}=1100-1600$ K). Reaction 7 is predicted to be the major route to CH_3SH as the alternative processes (i.e., reaction of either CH_3 and H_2S, or SH and CH_4, to produce CH_3SH and H) are thermodynamically unfavorable ($\Delta G_{reac}>0$) for $T_{gas}=1100-1600$ K. Table I shows that, at T_{gas}

>1600 K, CH_3SH can undergo successive H-abstraction reactions to yield CS (reaction 8). Although this overall process is much less thermodynamically favorable than the competing reaction 9 (attack by H to form CH_4 and SH), the initial abstraction of H (reaction 10) is favored. So once reaction 10 has occurred, successive abstractions of H will result in the formation of CS. This CS goes on to form CS_2 via (the favored) reaction 11.

Figure 7 illustrates the multistep conversion of CS_2 and H_2 in the HF reactor to reform H_2S and CH_4. This is in effect the reverse of overall reaction 1 which, although unfavorable for $T_{gas}>1200$ K, will be driven in the cooler regions of the reactor where H_2 and CS_2 concentrations are high (and are essentially the input gas mixture). Diffusion of the products into the hotter regions leads to the formation of CH_3 (the diamond growth species), thus allowing the deposition of diamond from such gas mixtures, as previously reported.[12] This process, whereby the input gases react prior to entering the hot region of the reactor, has many similarities with the mechanism for CH_3 production from HF activated C_2H_2/H_2 gas mixtures proposed in Ref. 38.

It is interesting to note that, despite the high input concentration of CS_2 in the 1% CS_2/H_2 gas mixture, no CS was detected in either the HF or MW MBMS experiments (Fig. 7). The reason for this may be that T_{gas} is lower for the 1% CS_2/H_2 plasma than the H_2S/1% CH_4/H_2 plasmas. This is indicated by the larger size of the plasma ball in the former case (at a fixed power input) resulting in a lower power density, and thus a lower average temperature, within the plasma. The formation of CS from CH_3SH (reaction 8) becomes unfavorable for $T_{gas}<1200$ K. The uncertainty in the calculation of ΔG_{reac} for this reaction is ~ 40 kJ mol^{-1}, corresponding to an error of ~ 200 K in the temperature quoted above. Reaction 8 is thus calculated to become unfavored thermodynamically within the range $1000<T_{gas}<1400$ K. If the outlying regions of the 1% CS_2/H_2 plasma are within this temperature range, then the reverse reaction now becomes spontaneous. The resultant CH_3SH then reacts with atomic H to produce CH_4 and SH (reaction 9). The residual HS radicals formed within the 1% CS_2/H_2 MW plasma (via reaction 2 and the reverse of reaction 7) could then diffuse to the cooler regions of the chamber and react to form S and S_2 (see reactions 3 and 4), leading to the observed sulfur deposition on the cool chamber wall.

Deposition from a 0.5% CS_2/H_2 MW plasma yielded a diamond film of good crystal quality, containing $\sim 0.05\%$ sulfur (as detected by XPS) but with a resistivity significantly greater than that measured for the H_2S grown examples. This indicates that in this case either (a) the S had not been incorporated into the diamond lattice in an electronically active form, or (b) there were an even greater number of compensating defects and acceptor states. This provides further evidence for the role of CS as a route to electronically active sulfur incorporation, since no CS was detected by MBMS in the CS_2/H_2 plasma (as discussed above).

V. CONCLUSIONS

H_2S has been added to 1% CH_4/H_2 gas mixtures in both HF and MW activated CVD. Little effect on film morphology or growth rate was observed for HF grown diamond films, even at high doping levels (1% H_2S in the gas phase), and little or no evidence was seen for S incorporation into these films. In contrast, deposition from MW plasmas yielded diamond films of which the morphology, degree of S incorporation, and electrical resistivities all varied with the level of H_2S addition.

Detailed investigations of the gas composition in both MW and HF reactors using MBMS techniques have provided new insights into the fundamental chemistry occurring in the gas phase. A mechanistic interpretation of these experimental results has been proposed, using simple thermodynamic considerations, which accounts for the observed differences between the HF and MW diamond deposition techniques.

The present study suggests that CS may be responsible for the incorporation of S into the diamond lattice of CVD films grown from H_2S/1% CH_4/H_2 gas mixtures, and that the production of CS is crucially dependent upon the volume of gas that can attain a sufficient T_{gas} for both the production of CS_2 and the subsequent buildup of CS to take place. This suggests that one route to larger S incorporation levels would be to use higher power MW systems or hotter deposition processes, such as arc jets, in which large volumes of gas acquire the necessary T_{gas}.

However, even with S incorporation levels of 0.2%, the polycrystalline films were too resistive to be useful for electronic devices. This does not rule out the possibility that S may be acting as a true *n*-type dopant, however, since it is possible that in these polycrystalline films there are a great many defects which could act as compensating acceptors, soaking up the donated electrons from the S. Thus the films appear to be much more resistive than would normally be expected for a truly *n*-doped material. Unless this problem is solved, the implementation of S-doped diamond may be limited to single crystal homoepitaxial films, for which conductivities and carrier mobilities may be sufficient to allow the fabrication of useful electronic devices.

ACKNOWLEDGMENTS

The authors would like to thank the EPSRC for project funding and De Beers Industrial Diamond, Ltd. for financial support (J.R.P.). Thanks also go to Sean Pearce, Dr. Jason Riley, Dudley Shallcross, Dr. Jeremy Harvey, Dr. Jonathan Hayes, Pippa Hawes, Les Corbin, and staff at the IAC at Bristol for their many and varied contributions to aspects of this work. The authors also wish to thank Professor Richard Jackman and Dr. Oliver Williams (at UCL), Professor Gehan Amaratunga and Nalin Rupesinge (Cambridge), and Professor Wang Wang and Dr. Sergei Stepanov (Bath) for their efforts at electrical and Hall measurements. P.W.M. also wishes to thank Dr. Toshihiro Ando and Dr. Mikka Nishitani-Gamo (NIRIM, Japan) for XPS and other measurements performed on the HF samples.

[1] K. E. Spear and J. P. Dismukes, *Synthetic Diamond, Emerging CVD Science and Technology* (Wiley, New York, 1994).
[2] P. W. May, Philos. Trans. R. Soc. London, Ser. A **358**, 473 (2000).
[3] M. N. Latto, D. J. Riley, and P. W. May, Diamond Relat. Mater. **9**, 1181 (2000).
[4] V. I. Polyakov, A. I. Rukovishnikov, N. M. Rossukanyi, A. I. Krikunov, V. G. Ralchenko, A. A. Smolin, V. I. Konov, V. P. Varnin, and I. G. Teremetskaya, Diamond Relat. Mater. **7**, 821 (1998).
[5] N. Vinocur, B. Miller, Y. Avyigal, and R. Kalish, J. Electrochem. Soc. **143**, L238 (1996).
[6] R. G. Farrer, Solid State Commun. **7**, 685 (1969).
[7] A. Reznik, C. Uzan-Saguy, R. Kalish, S. Mita, A. Sawabe, S. Koizumi, M. Kamo, and Y. Sato, Diamond Relat. Mater. **7**, 540 (1998).
[8] S. Bohr, R. Haubner, and B. Lux, Diamond Relat. Mater. **4**, 133 (1995).
[9] J. F. Prins, Mater. Sci. Rep. **7**, 271 (1992).
[10] S. Prawer, C. Uzan-Saguy, G. Braunstein, and R. Kalish, Appl. Phys. Lett. **63**, 2502 (1993).
[11] M. Hasegawa, D. Takeuchi, S. Yamanaka, M. Ogura, H. Watanabe, N. Kobayashi, H. Okushi, and K. Kajimura, Jpn. J. Appl. Phys., Part 2 **38**, L1519 (1999).
[12] G. D. Barber and W. A. Yarbrough, J. Am. Ceram. Soc. **80**, 1560 (1997).
[13] I. Sakaguchi, M. N. Gamo, Y. Kikuchi, E. Yasu, and H. Haneda, Phys. Rev. B **60**, R2139 (1999).
[14] M. N. Gamo, E. Yasu, C. Xiao, Y. Kikuchi, K. Ushizawa, I. Sakaguchi, T. Suzuki, and T. Ando, Diamond Relat. Mater. **9**, 941 (2000).
[15] M. N. Gamo, C. Xiao, Y. Zhang, E. Yasu, Y. Kikuchi, I. Sakaguchi, T. Suzuki, Y. Sato, and T. Ando, Thin Solid Films **382**, 113 (2001).
[16] R. Kalish, A. Reznik, C. Uzan-Saguy, and C. Cytermann, Appl. Phys. Lett. **76**, 757 (2000).
[17] T. Ando (private communication).
[18] D. S. Dandy, Thin Solid Films **318**, 1 (2001).
[19] W. L. Hsu, J. Appl. Phys. **72**, 3102 (1992).
[20] C. A. Rego, P. W. May, C. R. Henderson, M. N. R. Ashfold, K. N. Rosser, and N. M. Everitt, Diamond Relat. Mater. **4**, 770 (1995).
[21] R. S. Tsang, C. A. Rego, P. W. May, J. Thumin, M. N. R. Ashfold, K. N. Rosser, C. M. Younes, and M. J. Holt, Diamond Relat. Mater. **5**, 359 (1996).
[22] C. A. Rego, R. S. Tsang, P. W. May, M. N. R. Ashfold, and K. N. Rosser, J. Appl. Phys. **79**, 7264 (1995).
[23] R. S. Tsang, P. W. May, M. N. R. Ashfold, and K. N. Rosser, Diamond Relat. Mater. **7**, 1651 (1998).
[24] S. M. Leeds, P. W. May, E. Bartlett, M. N. R. Ashfold, and K. N. Rosser, Diamond Relat. Mater. **8**, 1377 (1999).
[25] S. M. Leeds, P. W. May, M. N. R. Ashfold, and K. N. Rosser, Diamond Relat. Mater. **8**, 226 (1999).
[26] J. R. Petherbridge, P. W. May, S. R. J. Pearce, K. N. Rosser, and M. N. R. Ashfold, J. Appl. Phys. **89**, 1484 (2001).
[27] *Handbook of X-ray Photoelectron Spectroscopy*, edited by J. Chastain (Perkin-Elmer, Minnesota, 1992).
[28] P. E. J. Flewitt and R. K. Wild, *Physical Methods of Materials Characterisation* (Institute of Physics, Bristol, 1994).
[29] S. M. Sze, *Physics of Semiconductor Devices* (Wiley, New York, 1981).
[30] S. M. Leeds, T. J. Davis, P. W. May, C. D. O. Pickard, and M. N. R. Ashfold, Diamond Relat. Mater. **7**, 233 (1998).
[31] A. K. Kulkarni, K. Tey, and H. Rodrigo, Thin Solid Films **270**, 189 (1995).
[32] B. J. Garrison, E. J. Dawnkaski, D. Srivastava, and D. W. Brenner, Science **255**, 835 (1992).
[33] S. J. Harris and D. G. Goodwin, J. Phys. Chem. **97**, 23 (1993).
[34] J. A. Smith, M. A. Cook, S. R. Langford, S. A. Redman, and M. N. R. Ashfold, Thin Solid Films **368**, 169 (2000).
[35] A. Gicquel, K. Hassouni, Y. Breton, M. Chenevier, and J. C. Cubertafon, Diamond Relat. Mater. **5**, 366 (1996).
[36] J. R. Petherbridge, P. W. May, G. M. Fuge, and M. N. R. Ashfold, Diamond Relat. Mater. (to be published).
[37] P. W. Atkins, *Physical Chemistry*, 2nd ed. (Oxford University, New York, 1984).
[38] J. A. Smith, E. Cameron, M. N. R. Ashfold, Y. A. Mankelevich, and N. V. Suetin, Diamond Relat. Mater. **10**, 358 (2001).
[39] M. W. Chase, Jr., J. Phys. Chem. Ref. Data, Monograph No. 9, Parts 1 and 2 (1998).
[40] J. N. Harvey (private communication).